Engineered Science
DOI: https://dx.doi.org/10.30919/es1329

Development and Performance Analysis of an Electromagnetic Needle-Free Jet Injection Device for Efficient Drug Delivery in Pig Farms

Sarasin Khotthada,[1] Anirut Matthujak,[1,*] Pracha Khamphakdi,[2] Jinda Glinubon,[3] Chawalit Siriboon,[3] Intr Salangam[3] and Sutthisak Phongthanapanich[4]

Abstract

This research addresses the challenges of traditional needle-based injections in pig farms, such as syringe breakage, drug residue, and stress-induced handling, which compromise animal welfare and meat quality. The aim is to develop an electromagnetic needle-free jet injector to provide a safer and more efficient drug delivery method. The device was designed using an electromagnetic actuator and optimized through MATLAB simulations, Polyvinylidene Fluoride (PVDF) pressure sensors, and high-speed video imaging. The device generated a high-speed jet using electromagnetic fields and neodymium iron boron (NdFeB) magnets. Calibration and impact pressure measurements are adopted to validate its performance. Results showed that the injector can generate jet speed up to 225 m/s and impact pressures exceeding 35 MPa, meeting the thresholds for effective drug delivery. Both simulation and experimental data also confirmed the reliability of the device. The polyacrylamide gel and porcine tissue results indicate precise and consistent drug delivery. The key findings highlight the ability of the device to maintain sufficient impact pressure and jet speed, making it suitable for veterinary and human medical applications. High-speed video analysis reveals an essential jet behavior for effective drug delivery, robust performance, and deep tissue penetration. Finally, this research shows that the injector significantly improves drug delivery in pig farms, offering a viable alternative to traditional injections by reducing contamination risks and stress while enhancing efficiency.

Keywords: Electromagnetic Needle-free Injection; Pig farm; Jet speed; Impact pressure; Jet dispersion.
Received: 02 August 2024; Revised: 16 November 2024; Accepted: 21 November 2024.
Article type: Research article.

1. Introduction

Efficient and safe drug delivery is essential in both veterinary and human medicine. Traditional needle-based injections in pig farms pose several significant challenges, including syringe breakage, drug residue in meat, and stress-induced handling. These issues not only compromise animal welfare and meat quality but also result in economic losses and increase the risk of infections and injuries to farm workers.[1-5] Consequently, there is a pressing need for innovative solutions that enhance the efficiency and safety of drug administration in pig farms.

Needle-free jet injection (NFI) technology presents a promising alternative by delivering precise, consistent dosages without the use of needles, thereby reducing injury, contamination risks, and stress.[6-10] However, despite recent advancements, several challenges remain. Current needle-free systems often face limitations such as inconsistent drug delivery, inadequate penetration depth, and high manufacturing costs. Various NFI systems, including spring-loaded, gas-powered, battery-operated, and piezoelectric jet injectors, each have drawbacks. For instance, spring-loaded jet injectors, while cost-effective, offer limited control over injection parameters and suffer from spring fatigue over time.[11,12] Gas-powered injectors provide better control but are bulky and require gas canisters, limiting portability.[13-15] Although portable and user-friendly, battery-operated injectors face battery life and maintenance issues, often lacking the precision needed for consistent dosing.[16,17] Despite their high precision and control, Piezoelectric

[1] *Combustion and Jet Application Research Laboratory (CJARL), Department of Mechanical Engineering, Faculty of Engineering, Ubon Ratchathani University, 85 Sathonlamark Road, Warin Chamrap, Ubon Ratchathani, 34190, Thailand*
[2] *Power Electronics Laboratory, Department of Electrical and Electronics Engineering, Faculty of Engineering, Ubon Ratchathani University, 85 Sathonlamark Roetad, Warin Chamrap, Ubon Ratchathani, 34190, Thailand*

injectors are more expensive, complex, and suitable primarily for microliter-level doses.[18-20] Additionally, liquid jet injectors frequently struggle with maintaining consistent dosage and achieving uniform tissue dispersion, with safety concerns also arising from the complexity and risks associated with pyro-drive mechanisms.[21,22]

Electromagnetic injectors represent a significant advancement in NFI technology, addressing many of these limitations. For example, Taberner, Hogan, and Hunter developed a controllable needle-free jet injection device using a high-stroke linear Lorentz-force motor with feedback control. This device allows precise control over injection depth (up to 16 mm) and delivery volume (up to 250 μL), enabling continuous monitoring and modulation of jet speed for consistent injections into transparent gels and post-mortem animal tissue.[23] Chang, Hogan, and Hunter further demonstrated that electromagnetic injectors could precisely control jet speed and impact pressure, ensuring minimal tissue damage and high accuracy in fluid sampling. Their system maintained a jet speed of up to 100 m/s with an accuracy of ± 5%.[24] Sripanagul *et al.* highlighted that electromagnetic actuators could generate water jets at speeds up to 150 m/s with precise control over force and direction, showcasing their versatility and effectiveness.[25,26] Huang *et al*. emphasized the high control and precision of electromagnetic injectors, making them ideal for delicate applications such as in-ovo vaccinations. These injectors achieved a penetration depth of 1.5 mm with uniform vaccine distribution, which is crucial for effective immunization in avian species.[27] However, current research has primarily focused on specific applications like fluid sampling and in-ovo vaccinations, leaving a need for devices optimized for livestock, particularly in achieving consistent performance across varying tissue types, optimizing design parameters for large animals, and ensuring practical usability in farm environments.

This research aims to address these gaps by developing an electromagnetic needle-free jet injector specifically designed for efficient vaccine delivery in pig farms. Our innovative device utilizes an electromagnetic actuator as the power source and integrates MATLAB simulations, pressure sensors, and high-speed video imaging to optimize design parameters and ensure precise drug delivery. This study provides practical insights into the device's performance through a comprehensive analysis of jet behavior, impact pressure, jet speed, and validation via simulations and experimental measurements. The results obtained in simulated and natural tissue environments highlight the potential of this device to revolutionize drug delivery practices in veterinary and human medicine. This study paves the way for safer, more efficient, and needle-free drug administration methods, demonstrating the device's efficacy and addressing existing gaps in current technologies.

By focusing on both simulation and experimental validation, we aim to demonstrate the device's capability to achieve high-impact pressures and jet velocities necessary for effective drug delivery. The results from simulated and natural tissue environments will highlight the potential of this technology to revolutionize drug delivery practices, offering a viable alternative to traditional injections by reducing contamination risks and stress while enhancing efficiency.

2. Research methodology

The objective of this research was to design and develop a needle-free jet injection device using an electromagnetic actuator as the power source. The device was designed based on the principle of impact driving method.[25,26,28] In addition, MATLAB simulations, a Polyvinylidene Fluoride (PVDF) pressure sensor, and high-speed video imaging were used to optimize design parameters, calibrate the equipment, and analyze the jet behavior.

2.1 Device components and working principle

The operation of the electromagnetic needle-free jet injection device begins with the controller sending a low-power electrical signal to an amplifier, which boosts the signal to a high-power level. This amplified signal is then sent back to the controller for precise regulation, ensuring accurate control over the actuator, as illustrated in Fig. 1.

Figure 2 depicts the sequence of events in the actuator setup ready for injection, including the bobbin, coil, NdFeB magnet, piston rod, piston, and nozzle. The actuator comprises copper coils wrapped around a bobbin and permanent NdFeB magnets, as shown in Fig. 2 (a). Before injection, the required volume of the liquid drug is pre-filled into the injector, ensuring the precise dosage is delivered. When the high-power signal energizes the copper coils, they generate an electromagnetic field that interacts with the magnetic field of the NdFeB magnets, as depicted in Fig. 2(b). This interaction moves the magnets, driving a plunger inside the nozzle and pushing the liquid drug through a small hole in the nozzle to form a high-speed jet, as shown in Fig. 2(c). This process ensures that the drug is expelled at high speed, enabling precise and efficient drug delivery without needles.

The motion of the plunger inside the nozzle, driven by electromagnetic interaction, plays a crucial role in generating the high-speed jet. The applied voltage with higher voltages leads to greater acceleration and higher jet velocities, directly affecting the plunger's speed and acceleration. This relationship is essential for accurately calculating the ejected volume. Due to the small nozzle aperture, the plunger initially moves at a different speed than the magnet; however, after

[3] *Department of Animal Science, Faculty of Agriculture, Ubon Ratchathani University, 85 Sathonlamark Road, Warin Chamrap, Ubon Ratchathani, 34190, Thailand*

[4] *Department of Mechanical Engineering Technology, King Mongkut's University of Technology North Bangkok, Bangsue, Bangkok, 10800, Thailand*

**Email:* anirut.m@ubu.ac.th, anirut.mat@gmail.com (A. Matthujak)

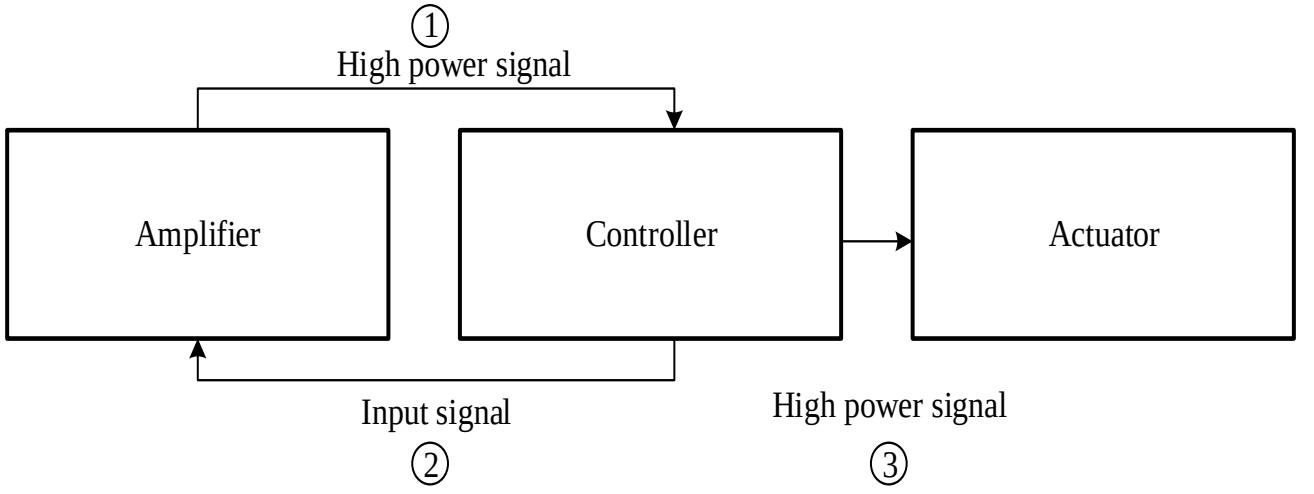

Fig. 1 Block diagram of electromagnetic needle-free jet injection device operation.

impact, the plunger and magnet move together at the same speed. Our device operates in single-shot mode, with each activation of the electromagnetic actuator producing a single high-speed jet pulse. This precise control over jet formation ensures consistent and accurate drug delivery, making the device well-suited for various medical applications.

Finally, we may summarize that the device leverages the principles of electromagnetism, combining high-power signal amplification with controlled electromagnetic interaction to form a high-speed drug jet, offering a needle-free solution for drug administration.

2.2 Simulation and calibration

In needle-free jet injection, the drug must be transformed into a high-speed jet with an impact pressure exceeding 15 MPa or velocities between 100 and 200 m/s to penetrate the skin.[23,29] This research conducted a comprehensive MATLAB simulation study to achieve these criteria and optimize the performance of the electromagnetic needle-free jet injection device. The goal is to ensure the impact pressure or jet speed

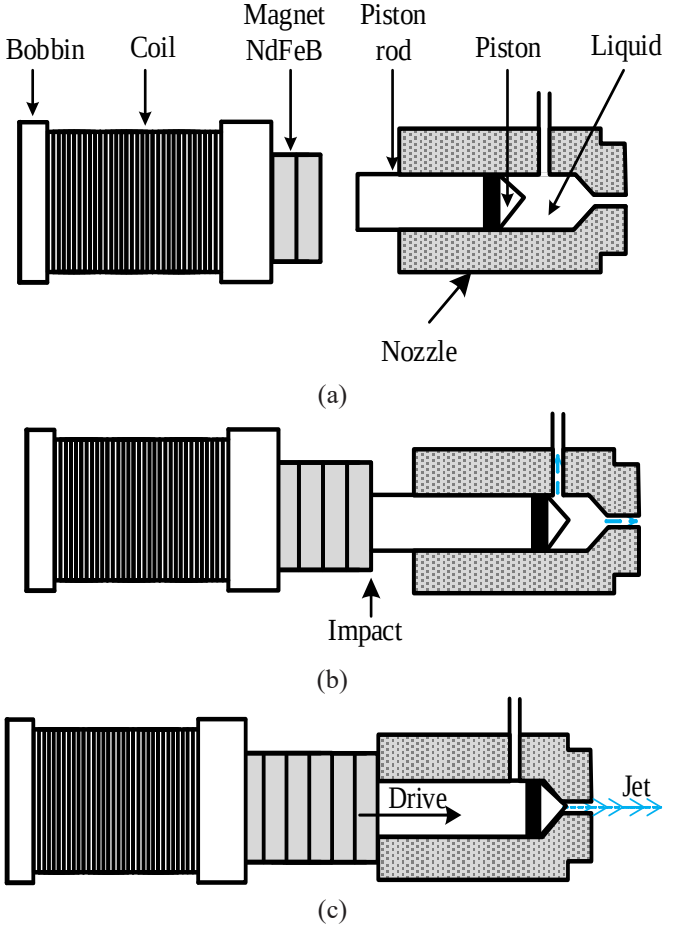

Fig. 2 Impact method for jet generation. (a) Before moving impact; (b) During moving impact; and (c) During moving impact.

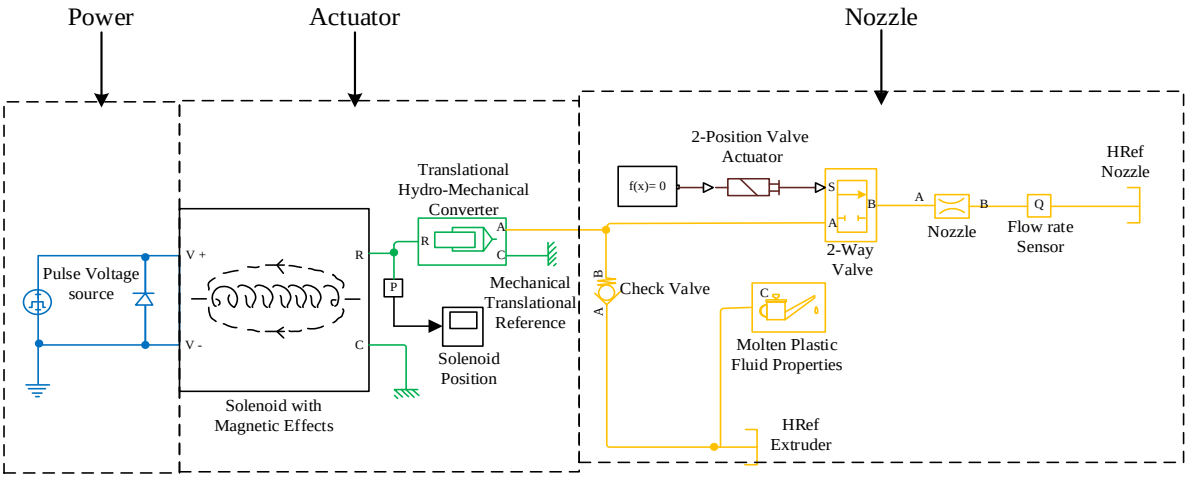

Fig. 3 Simulink model in MATLAB of the electromagnetic needle-free jet injector.

meets the necessary thresholds under various operating conditions, focusing on the power supply, actuator, and nozzle components.

Figure 3 illustrates a Simulink model of the electromagnetic needle-free jet injector in MATLAB, detailing its three main sections: Power, Actuator, and Nozzle. This integrated system is designed to optimize needle-free drug delivery, enhancing efficiency and safety in veterinary applications, particularly in pig farms.

The Actuator section includes a solenoid that converts electrical energy into mechanical motion. When energized by the pulse voltage, the solenoid creates a magnetic field that interacts with its core, producing mechanical motion. A hydro-mechanical converter translates this motion into the force needed to drive the piston within the nozzle. Accurate control of the solenoid position is essential for generating a high-speed jet capable of penetrating tissue, which is a crucial part of the working principle of the device.

The Nozzle section, responsible for the actual drug delivery, includes a 2-position valve actuator, a check valve to ensure proper fluid flow and a flow rate sensor for feedback control. The nozzle, with a diameter of 0.2 mm, creates a high-speed jet necessary for effective drug penetration and accommodates a drug volume of 100-500 µL.[12,30] The molten plastic fluid properties component ensures the fluid is at the correct viscosity and temperature for injection, while the HiEff extruder nozzle generates the required high-speed jet.

Table 1. Parameters for optimized product design.

Components	Parameters	Value
Power part	Direct current (DC) Voltage	50-250 V
	Frequency	50 Hz
Actuator part	Magnetic field strength	1.2 T
	Coil	1000 rev
Nozzle part	Nozzle diameter	0.2 mm
	Drug volume	100-500 µL

Various scenarios were tested in the Simulink model by adjusting parameters such as pulse voltage, solenoid position, and fluid flow rate to observe their effects on impact pressure and jet speed. Results showed that impact pressure and jet speed increased with higher input voltages. Moreover, optimal operating conditions were identified to ensure consistent and efficient drug delivery, as listed in Table 1. These parameters serve as the main guidelines for constructing the injection device, as shown in Fig. 4.

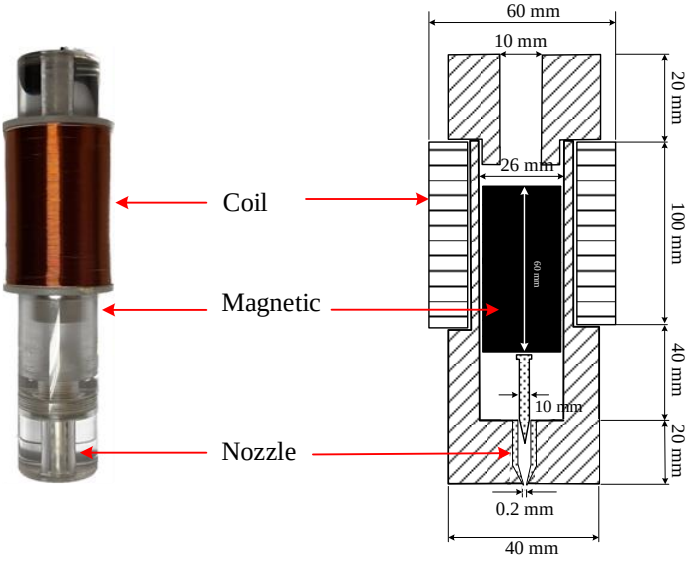

Fig. 4 Injection device.

2.3 Impact pressure and jet speed measurements

Specific methodologies and equipment were employed to measure the impact pressure and speed of the jet precisely. A PVDF sensor was utilized to measure impact pressure. The PVDF sheet, measuring 15 mm in width, 25 mm in length, and 28 µm in thickness, was mounted on a Polymethyl Methacrylate (PMMA) block with dimensions of 45 × 45 mm² and a thickness of 25 mm, as shown in Fig. 5. Moving towards the PVDF sheet, the jet strikes it at a stand-off distance of 3 mm. The PVDF sensor responds to the jet impact by generating an electrical signal, which is displayed on a digital oscilloscope as a voltage signal (V_e). This voltage is then used

to calculate the impact pressure of the jet, as shown by Eq (1). The calibration relies on the principle of momentum balance, where known masses were dropped from varying heights, and the resulting impact on the PVDF sensor was recorded to establish a precise voltage-to-pressure relationship.

$$P = 23.691V_e \quad (1)$$

where P is impact pressure (MPa), and V_e is a voltage signal (V) obtained by a digital oscilloscope.

For speed measurement, a high-speed video camera (Protron Fastcam Mini UX 50) operating at 10,000 frames per second (fps) and an exposure of 1/20000 with a resolution of 640 × 240 pixels was used. By capturing the jet motion, as depicted in Fig. 6, the speed of the jet was calculated using the footage and applying the relevant Eq (2).

$$V_j = \frac{\Delta s}{\Delta t} \quad (2)$$

where V_j is the jet speed (m/s), Δs is the jet penetration distance (m), and Δt is the time obtained from a high-speed video camera (s).

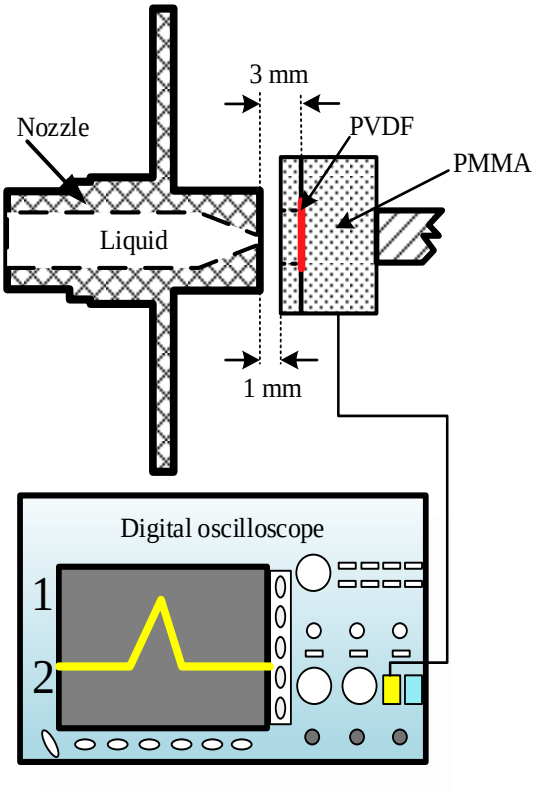

Fig. 5 Impact pressure measurement setup.

These methods ensure accurate measurement of the critical parameters, such as impact pressure and speed, which are essential for evaluating the performance of the electromagnetic needle-free jet injection device. Moreover, the combination of PVDF sensors and high-speed video analysis provides a comprehensive understanding of the jet dynamics, confirming the effectiveness of the device in delivering drugs efficiently.

2.4 Simulated tissue and porcine tests

A series of tests were conducted on both simulated and actual porcine tissue to validate the performance and efficacy of the electromagnetic needle-free jet injection device. Polyacrylamide gel was adopted as the simulated tissue test due to its transparency and mechanical properties, which are similar to human tissue. Specifically, a 20% concentration of polyacrylamide gel, with Young's modulus ranging from 0.22 to 0.38 MPa, was used.[12,29,30] The preparation involved mixing 25 mL of 40% Acrylamide stock with 25 mL of distilled water, then adding 0.2 mL of APS and 0.2 mL of Tetramethylethylenediamine (TEMED) to initiate polymerization. This setup allowed clear and precise observation of jet dispersion and penetration, which are critical for assessing the performance in a controlled environment.

In our jet dispersion experiments with polyacrylamide gel at 250 V, we carefully controlled the injected volume independently of the applied voltage. This was achieved by pre-filling the injector with a set volume of the dye solution before each test, ensuring that volume adjustments did not affect the voltage or pressure applied during the injection. The dye used for visualization was methylene blue, selected for its clear contrast in the gel medium, allowing for an accurate assessment of jet dispersion patterns. Additionally, to facilitate comparison with previous studies, we measured and reported the Young's modulus of the polyacrylamide gel phantoms, approximately 0.22-0.38 MPa, aligning with properties reported for similar phantoms used in jet penetration studies. A scale bar has also been added to the figure for precise spatial reference. These details provide a comprehensive understanding of the experimental setup and conditions used in our study.

The device was also tested on porcine tissue from a 4-week-old crossbred finishing pig (Duroc × Large White × Landrace), commonly raised in Thai pig farms. The tests were conducted on the neck area of the pig carcass, a common site for vaccine administration in livestock. These tests aimed to observe the penetration depth, dispersion pattern, and overall

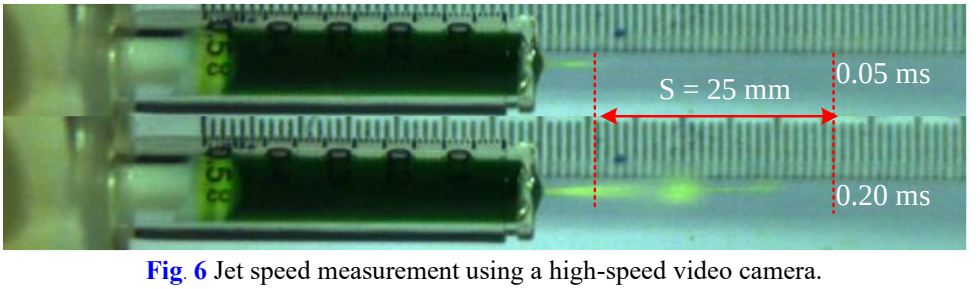

Fig. 6 Jet speed measurement using a high-speed video camera.

effectiveness of the jet in delivering the drug within muscle tissue.

Combining simulated tissue and pork tests comprehensively evaluated the device's capabilities. The polyacrylamide gel test offered insights into the jet behavior in a controlled setting, while the porcine tissue test demonstrated the practical applications in a realistic scenario. These tests confirmed the ability to achieve precise and efficient drug delivery, highlighting its potential for improving vaccination practices in pig farming and possibly extending to human medical applications.

3. Results and discussion

3.1 Simulation and experimental validation

Simulations and experimental measurements were conducted to validate the performance of the electromagnetic needle-free jet injection device and identify conditions yielding an impact pressure exceeding 35 MPa. This condition is essential because effective skin penetration in needle-free jet injection requires transforming the drug into a high-speed jet with an impact pressure exceeding 15 MPa or velocities between 100 and 200 m/s.[23,29] The goal is then to determine the optimal parameters for efficient device performance.

Simulations involved a jet beam setup with a 0.2 mm nozzle and applying voltage in the 50 to 250 V range to predict impact pressure. The aim is to achieve impact pressures above 35 MPa. Experimental measurements used a PVDF sensor to capture the jet impact pressure. Jets were generated at voltages of 50, 100, 150, 200, and 250 V, and the PVDF sensor, connected to a digital oscilloscope, provided voltage signals calibrated to measure impact pressure accurately.

Figure 7 illustrates the relationship between voltage and impact pressure of the device. Simulation and experimental data show that impact pressure also rises as voltage increases. At lower voltages (50-100 V), the impact pressure remains below 10 MPa. However, it increases significantly at higher voltages.

The comparison between simulation data and experimental data shows a strong correlation. At 50 V, both results show minimal impact pressure. At 100 V, the simulation predicts slightly higher impact pressure than experimental results, but the difference is negligible. The results converge closely at higher voltages, *e.g.*, 200-250 V, indicating substantial agreement between the model and real-world performance. The maximum impact pressure recorded from simulations was 39.66 MPa at 250 V, while experimental measurements showed 37 MPa, indicating a 7% tolerance. Moreover, the average tolerance is around 8.53%. The close alignment of the results validates the benefit of using the Simulink model for device design and optimization.

Hence, the results, as explained above, confirmed that the electromagnetic needle-free jet injection device can achieve the necessary high-impact pressures for effective drug delivery. The strong correlation between simulation and experimental results underscores the reliability and efficiency of the device. This research also highlights the potential of electromagnetic NFI technology to revolutionize drug delivery in veterinary and human medical applications by providing the necessary parameters to optimize device performance, as shown in Table 1. Moreover, the experimental validation confirms that the optimal design parameters help apply to design an effective device that can penetrate the skin in real-world scenarios.

3.2 Jet performance in electromagnetic jet injection

Understanding the volume of liquid used in the electromagnetic needle-free jet injection device is crucial

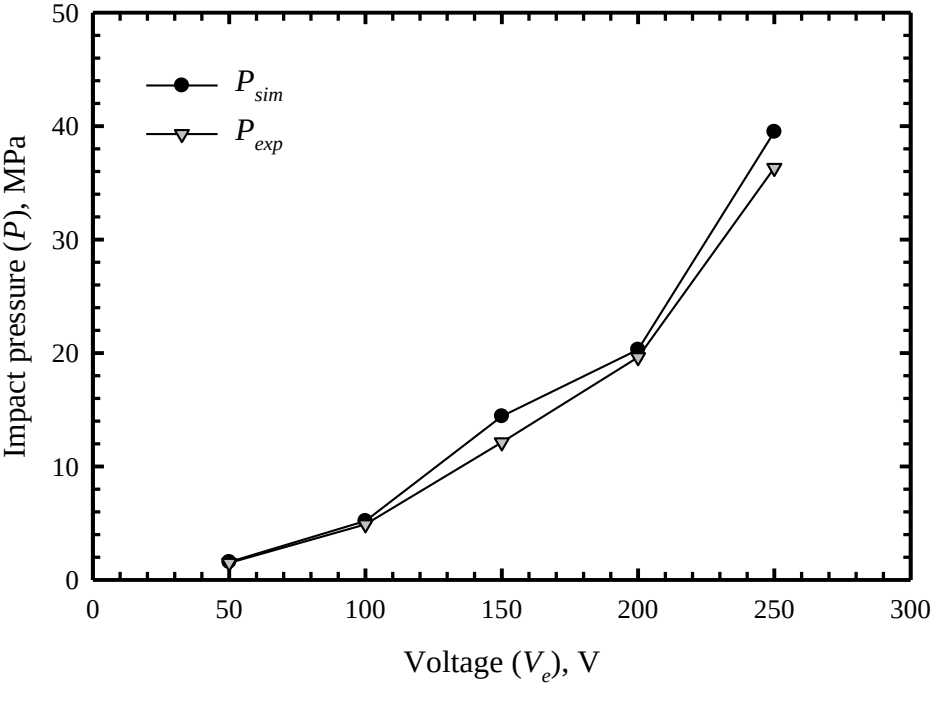

Fig. 7 Comparison of impact pressure obtained from simulation and experiment at various voltages.

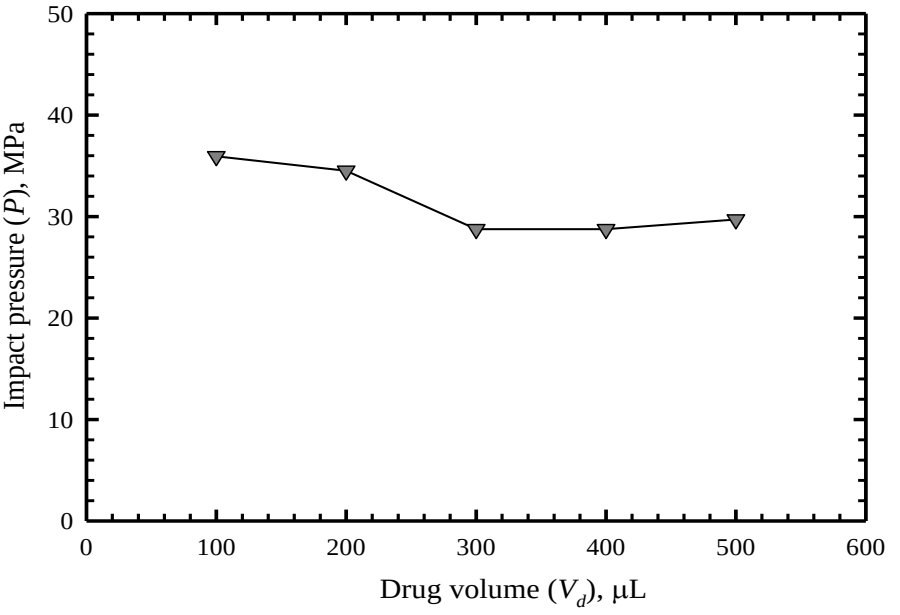

Fig. 8 Influence of drug volume on impact pressure at 250 V.

because different volumes represent different doses of drug delivery, significantly impacting the device performance, including impact pressure and efficacy of the delivery through pig skin. Studying these variations ensures the device can deliver drugs effectively across a range of doses in order to optimize its use in veterinary applications. In this investigation, 250 V was chosen as the maximum voltage to explore the upper limits of the device performance and ensure it can achieve the necessary impact pressures and velocities for effective drug delivery.

Figure 8 illustrates the influence of drug volume on the impact pressure of a water jet. The graph plots the impact pressure (P) in MPa against the drug volume (V_d) in μL, showing measured impact pressures for volumes ranging from 100 to 500 μL. As indicated, the impact pressure decreases as the drug volume increases. At 100 μL, the impact pressure peaks at approximately 37 MPa; however, at 500 μL, it is reduced to 30 MPa. This trend is due to the increased resistance the piston encounters as the liquid volume and mass rise. It is evident that when the mass of liquid increases, it exerts more force against the piston, reducing the efficiency of the force transfer that generates the jet. Despite this decrease, the impact pressure remains sufficiently high for effective penetration and drug delivery. An impact pressure exceeding 15 MPa is necessary to penetrate the skin, and the device can maintain pressure well above this threshold to show its efficacy. At 100 μL, the pressure of 37 MPa is significantly higher than required. However, at the volume of 500 μL, the pressure of 30 MPa is sufficient for effective penetration, indicating the robust device performance.

Figure 9 presents high-speed video frames showing the behavior of a water jet at a drug volume of 500 μL, captured at various time intervals. Initially, the liquid is at rest. Later, at t = 0.05 ms, the jet begins to form and exits the nozzle at high speed. At t = 0.1 ms, the jet extends further and maintains a coherent stream. As the jet progresses, a secondary jet forms by t = 0.2 ms, breaking into segments due to high-speed movement and air interaction. By t = 0.5 ms, a third jet appears, with further dispersion observed at t = 0.6 ms, showing a mist-like pattern as the liquid breaks into finer droplets. The high-speed video frames provide valuable insights into the jet dynamics produced by the electromagnetic needle-free jet injector. Initially forming a coherent stream, the jet breaks into segments and eventually disperses into fine droplets. The formation of secondary and tertiary jets indicates the high speed and energy required for effective drug delivery. This dispersion pattern ensures the drug can penetrate and spread within the target tissue, enhancing delivery efficacy.

In this analysis, the jet speed calculated from Fig. 9 is approximately 117 m/s, lower than the maximum claimed

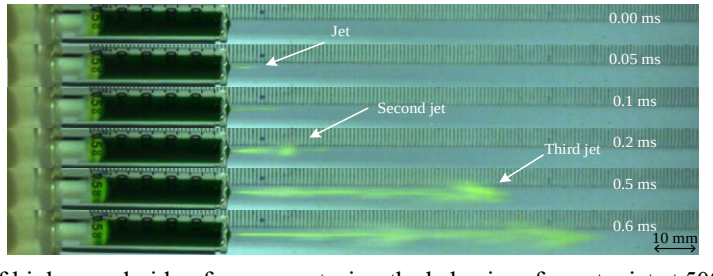

Fig. 9 Series of high-speed video frames capturing the behavior of a water jet at 500 μL and 250 V.

speed of 250 m/s. However, it is essential to note that effective skin penetration is influenced not only by jet speed but also by the impact pressure generated by the jet. The conditions under which our device operates ensure that, despite the reduced speed in this instance, the impact pressure remains high enough to achieve successful skin penetration. This is supported by experimental tests, as shown in Fig. 13, where injections into the skin were performed and confirmed effective under these specific conditions.

Figure 10 shows the influence of drug volume on jet speed for the electromagnetic needle-free jet injection device operating at 250 V. The graph plots jet speed (V_j) in meters per second (m/s) against drug volume (V_d) in microliters (μL), indicating measured jet velocities for varied volumes from 100 to 500 μL. As the graph indicates, jet speed decreases as the drug volume increases. At 100 μL, the jet speed peaks at approximately 225 m/s; at 500 μL, it is reduced to around 150 m/s. This decrease is due to the increased resistance the piston encounters with higher liquid volumes. Therefore, we may conclude that when the mass of liquid increases, it exerts more force against the piston, reducing the efficiency of the force transfer that generates the jet.

Despite the decrease in jet speed with larger drug volumes, the speed remains sufficiently high for effective penetration and drug delivery. Achieving a jet speed between 100 and 200 m/s or an impact pressure exceeding 15 MPa is essential to penetrate the skin. The device's efficacy is ensured due to its ability to maintain speed well above this threshold. We also found that at 100 μL, the speed of 225 m/s is significantly higher than required. However, at 500 μL, the speed of 150 m/s is sufficient for effective penetration, indicating the robust device performance.

These findings highlight the device's capability to maintain sufficient impact pressure and jet speed across various drug volumes, ensuring versatile application potential in veterinary and human medical fields. This performance underscores the ability to efficiently deliver medications through the skin, making it a viable alternative to traditional needle-based injections. Therefore, understanding how drug volume impacts jet speed helps refine the design and operation to achieve consistent and efficient drug delivery, ensuring both animal welfare and effective medication administration in pig farms. This analysis is crucial for optimizing the electromagnetic needle-free jet injection device, ensuring it can deliver drugs effectively across various doses in veterinary applications. Comparative analysis with existing studies on electromagnetic needle-free jet injectors demonstrates the unique performance characteristics of our device. For example, Sripanagul *et al.*[26] reported a maximum jet speed of 239.57 m/s and an impact pressure of 133.27 MPa in a water jet drilling application driven by an electromagnetic actuator under similar conditions. In contrast, other studies utilizing piezoelectric actuators achieved lower jet velocities with limited control over ejected volume. Our device's ability to achieve both high jet speed and controlled ejection volume while operating in single-shot mode offers a notable improvement in precision, which is particularly beneficial for veterinary applications where accurate dosage is critical. This comparison highlights the significance of our work in advancing needle-free jet injector technology through electromagnetic actuation, enabling greater flexibility and performance.

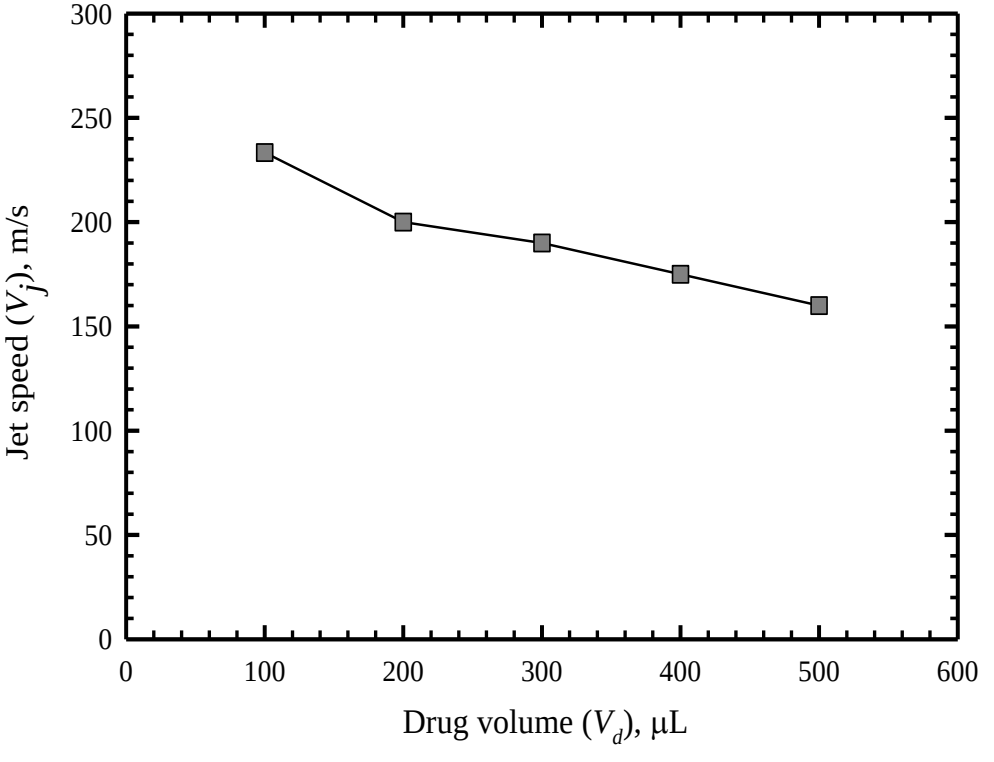

Fig. 10 Influence of drug volume on jet speed at 250 V.

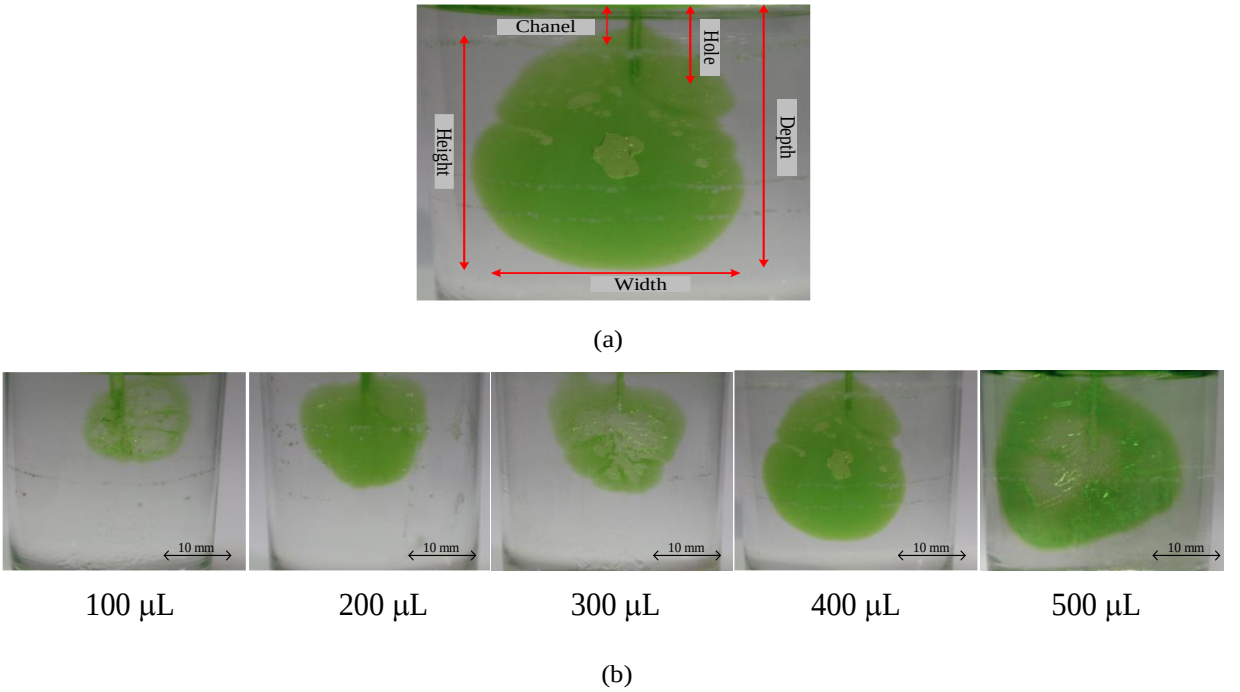

Fig. 11 Jet dispersion in polyacrylamide gel at 250 V (a) represents a single jet dispersion event with parameters such as channel depth and dispersion width; (b) represents a series of images showing jet dispersion for drug volumes ranging from 100 to 500 µL.

3.3 Jet penetration and dispersion in the simulated and porcine tissues

The analysis of impact pressure and jet speed demonstrates the robust performance of the electromagnetic needle-free jet injection device across various volumes. To further understand its efficacy, it is essential to investigate how the jet penetrates and disperses within tissues. This study examines jet penetration and dispersion in simulated polyacrylamide gel and actual porcine tissue, providing insights into the practical application and effectiveness in real-world scenarios.

Simulated tissues, such as polyacrylamide gel, offer a controlled environment to observe jet behavior and penetration without the complexities of biological variability. Porcine tissue, with its anatomical similarities to pig skin and muscle, serves as an excellent proxy for assessing performance in veterinary applications. By examining jet penetration and dispersion in these tissues, we can evaluate the uniformity of drug distribution, depth of penetration, and potential for tissue damage. These assessments are crucial for optimizing the device design and ensuring its reliability in delivering medications effectively and safely. The results will help determine if the device maintains sufficient impact pressure and speed to achieve the desired therapeutic outcomes, confirming its suitability as a viable alternative to traditional needle-based injections.

Figure 11 illustrates jet dispersion in polyacrylamide gel at 250 V, showcasing the performance across different drug volumes. In Fig. 11(a), a single jet dispersion event highlights key parameters such as channel (upper depth of dispersion), hole (penetration depth), width, height, and depth of the dispersed jet in the gel. These measurements are essential for quantifying the spread and penetration of the drug, which is critical for ensuring effective delivery. Fig. 11(b) presents a series of images showing jet dispersion for drug volumes ranging from 100 to 500 µL. As the drug volume increases, the dispersion pattern changes, indicating how the liquid interacts with the gel at different volumes. At 100 µL, the jet forms a small, concentrated area of dispersion, which becomes more prominent and more diffused at 500 µL. This trend aligns with earlier findings that increased liquid volume leads to broader dispersion.

Building on these findings, we also examined the effect of injected volume on jet speed, as increased volume can introduce additional fluid resistance within the nozzle, potentially reducing jet speed and, consequently, penetration depth. Therefore, optimizing both volume and speed is critical for achieving effective injection outcomes. To further evaluate injector performance, we have introduced jet power as an additional metric, as it provides a comprehensive measure of energy transfer during injection. Jet power offers insight into the force exerted by the jet and serves as a useful indicator of penetration potential.[31,32] Together, these metrics enhance our assessment of the device's effectiveness in delivering precise and controlled injections.

Figure 12 provides a jet penetration and dispersion in polyacrylamide gel at various water volumes. The graph measures penetration and dispersion in terms of channel, hole, width, height, and depth, each presented in millimeters (mm). The data shows a clear trend of increasing dispersion metrics with higher drug volumes. The channel parameter increases slightly with higher volumes, indicating broader initial jet entry into the gel. The hole parameter shows a noticeable

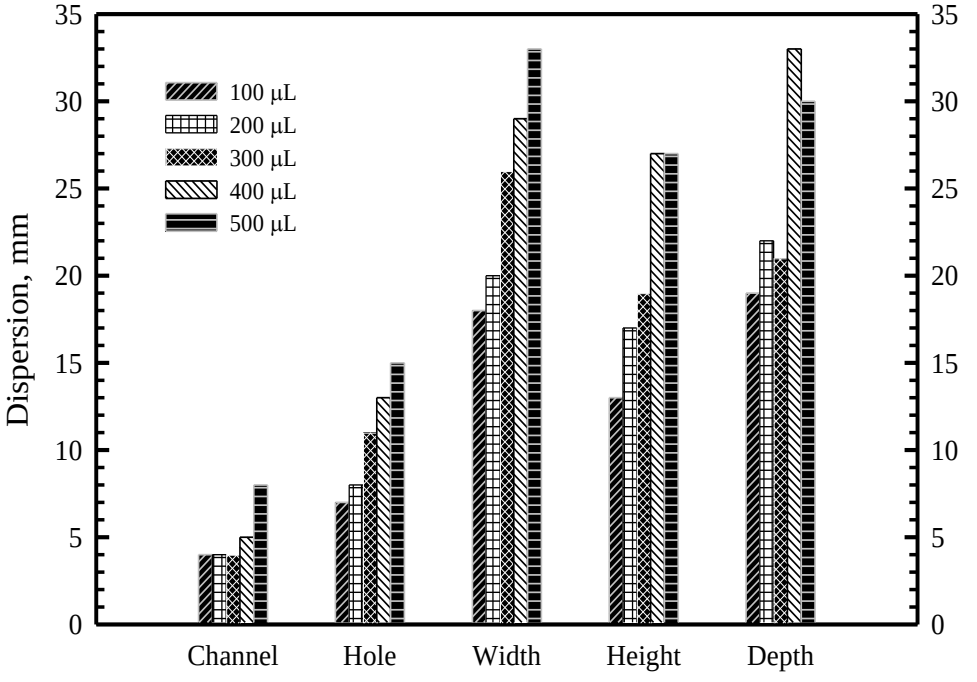

Fig. 12 Comparison of jet dispersion in polyacrylamide gel at various water volumes.

increase with higher volumes, suggesting a deeper initial impact. Width significantly increases with volume, reaching its peak at 500 µL, highlighting extensive lateral dispersion. Similarly, the dispersion height increases with drug volume, indicating a substantial vertical spread within the gel. Penetration depth increases consistently with volume, with the highest depth observed at 500 µL, underscoring the device's capability to penetrate deeper into the tissue.

Moreover, the study examined the penetration and dispersion characteristics of water jets in porcine tissue to confirm the practical application of the device. Fig. 13 illustrates the dispersion patterns in porcine tissue, showing how the jet penetrates and spreads at various drug volumes (100, 200, 300, 400, and 500 µL) at 250 V. Fig. 13(a) details key parameters such as channel, hole, width, height, and depth, similar to those in Fig. 11(a).

The porcine tissue includes layers representative of actual skin and muscle tissue. The outermost layer, the epidermis, serves as a protective barrier. At lower volumes, *e.g.*, 100 µL, the jet impact is concentrated near the surface, indicating penetration primarily in the epidermis and upper dermis. The middle layer, the dermis, contains connective tissues, blood vessels, and nerve endings. Penetration into this layer ensures the drug can be absorbed into the bloodstream and distributed throughout the body. As the volume increases, the jet penetrates deeper into the dermis, enhancing drug absorption and effectiveness. The innermost layer, the subcutaneous tissue, comprises fat and connective tissues, targeting deeper drug delivery. At higher volumes (400 and 500 µL), the jet penetrates through the dermis into the subcutaneous tissue, ensuring thorough drug dispersion and extended-release.

The green dye in the images illustrates drug penetration into these layers. At lower volumes, the dye is concentrated near the surface; however, with higher volumes, it penetrates deeper, reaching the lower dermis and subcutaneous tissue. This deep penetration ensures drug distribution throughout the targeted areas, enhancing the therapeutic effect. Effective penetration into all skin layers is critical for the versatility and reliability of the device to ensure the drug reaches its intended target, whether for vaccination, medication, or other therapeutic purposes. These findings highlight the potential of the device to replace traditional needle-based injections, providing a safer, more efficient method of drug delivery that minimizes infection risk and tissue damage.

To further assess the injector's performance, we calculated the jet power using established methods from the literature.[31,32] Jet power provides a comprehensive measure of the energy transfer during injection and is defined by the Eq. (3):

$$P = \frac{1}{2}\rho A V^3 \quad (3)$$

where P is the jet power (W), ρ is the fluid density (kg/m³), A is the nozzle cross-sectional area (m²), and V is the jet speed (m/s).

Given that the fluid is water (ρ = 1000 kg/m³) and the nozzle diameter is 0.2 mm (radius r = 0.1 mm = 10^{-4} m), the cross-sectional area is $A = \pi r^2 = \pi(0.0001)^2 = 3.14 \times 10^{-8}$ m². By using the maximum jet speed of 225 m/s, the jet power is calculated by the Eq. (4).

$$P = \frac{1}{2}(1000)(3.14 \times 10^{-8})(225)^3 = 179\ \text{W} \quad (4)$$

However, at a jet speed of 150 m/s, the jet power decreases to Eq. (5).

$$P = \frac{1}{2}(1000)(3.14 \times 10^{-8})(150)^3 = 53\ \text{W} \quad (5)$$

These calculations demonstrate that jet power increases

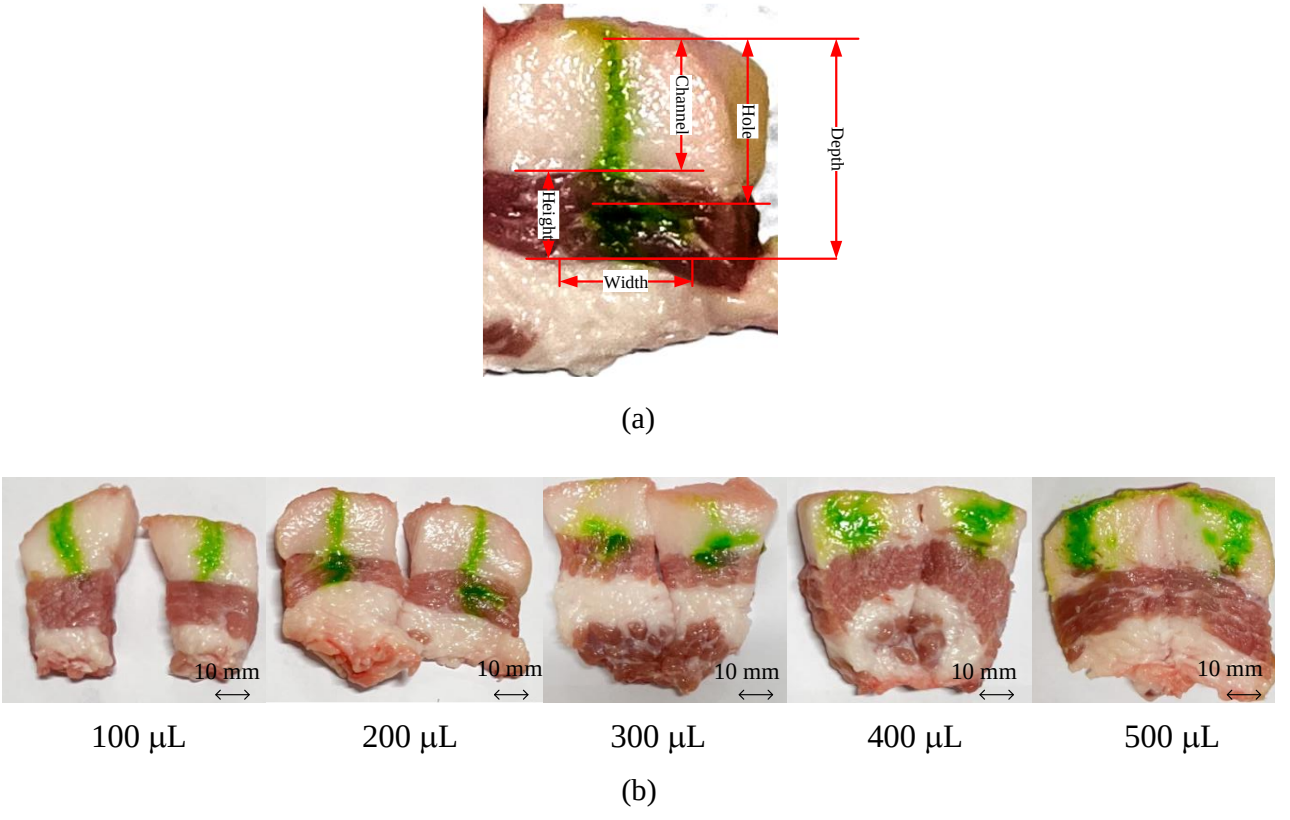

Fig. 13 Jet dispersion in porcine tissue at 250 V (a) represents dispersion patterns in porcine tissue with key parameters such as penetration depth; (b) represents the effects of varying drug volumes on the tissue.

significantly with jet speed. However, as the injected volume increases, jet speed decreases due to the added fluid mass and increased resistance within the nozzle, partly due to shock wave reflection.[33,34] This reduction in jet speed leads to a lower jet power, which can result in decreased penetration depth. This phenomenon explains the observed penetration depths and is consistent with previous studies.[31,32]

Figure 14 quantitatively presents the dispersion characteristics of the jet penetration and dispersion obtained in Fig. 13, highlighting that the channel depth and penetration depth (hole) reached their highest values at 200 μL. At this volume, the channel parameter, representing the upper depth of dispersion, peaked and then showed a decreasing trend with increasing liquid volume. Similarly, the hole parameter, indicating penetration depth, was also highest at 200 μL. The data shows a clear trend of increasing dispersion metrics with higher drug volumes. The channel parameter increases slightly with higher volumes, indicating a broader initial jet entry into the tissue. The hole parameter shows a more noticeable increase as the volume rises, suggesting a deeper initial impact with larger volumes. The width parameter significantly increases with volume, indicating that the jet spreads wider within the tissue as the drug volume increases, reaching its peak at 500 μL. Similarly, the dispersion height also increases with drug volume, indicating a substantial vertical spread within the tissue. The depth parameter, representing the maximum depth of dispersion, shows a significant increase at 200 μL, reaching up to 30 mm, and continues to increase with higher volumes, underscoring the capability to penetrate deeper into the tissue with larger volumes.

Understanding the dispersion and penetration characteristics in both simulated and real tissues allows for optimizing the design of the electromagnetic needle-free jet injection device. This optimization ensures effective and consistent drug delivery, enhancing animal welfare and improving medication administration efficiency in pig farms. The comprehensive analysis underscores the device's potential as a viable alternative to traditional injection methods, paving the way for advancements in both veterinary and human medical fields. Moreover, the device demonstrates its versatility and reliability by achieving consistent and extensive dispersion across different volumes, making it suitable for various medical and veterinary applications.

Finally, we want to remark that future studies should investigate long-term effects and potential tissue damage to ensure the safety and efficacy for clinical use.

4. Conclusions

This research addresses the challenges of traditional needle-based injections in pig farms, such as syringe breakage, drug residue in meat, and stress-induced handling, which compromise animal welfare and meat quality. We developed an electromagnetic needle-free jet injector as a safer, more efficient alternative for drug delivery. The device, designed using an electromagnetic actuator, was optimized through MATLAB simulations, pressure sensors, and high-speed video

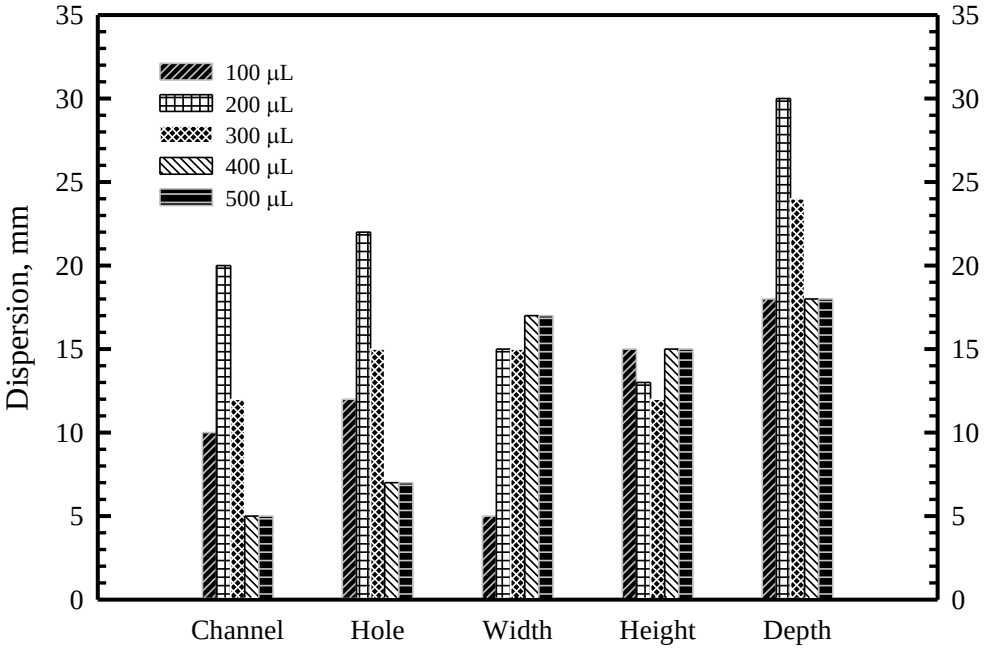

Fig. 14 Comparison of jet dispersion in porcine tissue at various water volumes.

imaging. The components and principles focused on using electromagnetic fields and NdFeB magnets to generate a high-speed jet. Calibration and impact pressure measurements with PVDF sensors and high-speed video analysis are adopted to validate its capability. The injector achieved jet velocities up to 225 m/s and impact pressures exceeding 35 MPa, meeting the necessary thresholds for effective drug delivery. Both simulations and experimental data showed a strong correlation that may confirm its reliability. The testing on polyacrylamide gel and porcine tissue also demonstrated precise and consistent drug delivery. The device maintained sufficient impact pressure and jet speed for versatile veterinary and human medicine use. High-speed video revealed dynamic jet behavior essential for effective drug delivery. The study confirmed the robust device performance by achieving deep tissue penetration and uniform drug distribution. This research significantly improves drug delivery in pig farms, offering a viable alternative to traditional injections by reducing contamination risks and stress while enhancing efficiency. They revealed consistent performance and practical usability, positioning it as a transformative tool in veterinary healthcare. Furthermore, future research should explore long-term effects and potential tissue damage for clinical safety. Optimizing design parameters for large-scale use and exploring human medical applications could further enhance its impact. However, the research should ensure the device consistently achieves impact pressures above 35 MPa and jet velocities up to 225 m/s to meet performance standards.

Acknowledgments

This research was financially supported by the Science Research and Innovation Promotion Fund (SRIPF) through the Fundamental Fund for the fiscal years 2022–2023 (Project Nos. 2355446 and 4161746).

Conflict of Interest

There is no conflict of interest.

Supporting Information

Not applicable.

References

[1] A. M. Erlendsson, M. Haedersdal, A. M. Rossi, Needle-free injection assisted drug delivery-histological characterization of cutaneous deposition, *Lasers in Surgery and Medicine*, 2020, **52**, 33-37, doi: 10.1002/lsm.23191.

[2] J. Imoto, T. Ishikawa, A. Yamanaka, M. Konishi, K. Murakami, T. Shibahara, M. Kubo, C.-K. Lim, M. Hamano, T. Takasaki, I. Kurane, H. Udagawa, Y. Mukuta, E. Konishi, Needle-free jet injection of small doses of Japanese encephalitis DNA and inactivated vaccine mixture induces, 2010, **28**, 7373-7380, doi: 10.1016/j.vaccine.2010.09.008.

[3] C. Jennissen, J. Wallace, K. Donham, D. Rendell, S. Brumby, Unintentional needlestick injuries in livestock production: a case series and review, *Journal of Agromedicine*, 2010, **16**, 58-71, doi: 10.1080/1059924x.2011.534045.

[4] R. Espinosa, D. Tago, N. Treich, Infectious diseases and meat production, *Environmental and Resource Economics*, 2020, **76**, 1019-1044, doi: 10.1007/s10640-020-00484-3.

[5] T. J. Tobias, J. C. M. Vernooij, A. van Nes, Comparison of efficacy of needle-free injection versus injection by needle for iron supplementation of piglets: a double blind randomized controlled trial, *Porcine Health Management*, 2023, **9**, 2, doi: 10.1186/s40813-022-00296-5.

[6] H. Li, Y. Shi, X. Ding, C. Zhen, G. Lin, F. Wang, B. Tang, X.

Li, Recent advances in transdermal insulin delivery technology: a review, *International Journal of Biological Macromolecules*, 2024, **274**, 133452, doi: 10.1016/j.ijbiomac.2024.133452.
[7] J. M. Rosselló, C.-D. Ohl, Bullet jet as a tool for soft matter piercing and needle-free liquid injection, *Biomedical Optics Express*, 2022, **13**, 5202, doi: 10.1364/boe.469486.
[8] M. Schlich, L. Casula, A. Musa, R. Pireddu, G. Pitzanti, M. C. Cardia, D. Valenti, S. Marceddu, A. M. Fadda, M. A. De Luca, C. Sinico, F. Lai, Needle-free jet injectors and nanosuspensions: exploring the potential of an unexpected pair, *Pharmaceutics*, 2022, **14**, 1085, doi: 10.3390/pharmaceutics14051085.
[9] M. A. Trimzi, Y.-B. Ham, A needle-free jet injection system for controlled release and repeated biopharmaceutical delivery, *Pharmaceutics*, 2021, **13**, 1770, doi: 10.3390/pharmaceutics13111770.
[10] A. D. Ravi, D. Sadhna, D. Nagpaal, L. Chawla, Needle free injection technology: A complete insight, *International journal of pharmaceutical investigation*, 2015, **5**, 192-199, doi: 10.4103/2230-973X.167662.
[11] V. Z. Bekkers, L. Bik, J. C. van Huijstee, A. Wolkerstorfer, E. P. Prens, M. B. A. van Doorn, Efficacy and safety of needle-free jet injector-assisted intralesional treatments in dermatology-a systematic review, *Drug Delivery and Translational Research*, 2023, **13**, 1584-1599, doi: 10.1007/s13346-023-01295-x.
[12] D. Zeng, N. Wu, L. Xie, X. Xia, Y. Kang, An experimental study of a spring-loaded needle-free injector: influence of the ejection volume and injector orifice diameter, *Journal of Mechanical Science and Technology*, 2019, **33**, 5581-5588, doi: 10.1007/s12206-019-1051-1.
[13] P. Hankare, A. Agrawala, V. Menezes, High-speed jet injector for pharmaceutical applications, *Journal of Medical Devices*, 2022, **16**, 034502, doi: 10.1115/1.4054549.
[14] R. Portaro, J. Sadek, H. Xu, H. D. Ng, Controlled release using gas detonation in needle-free liquid jet injections for drug delivery, *Applied Sciences*, 2019, **9**, 2712, doi: 10.3390/app9132712.
[15] Y. Zhu, C. Kang, W. Cai, C. Huang, Drug injection and dispersion characteristics of an air-powered needle-free injector, *Medical Engineering & Physics*, 2022, **109**, 103906, doi: 10.1016/j.medengphy.2022.103906.
[16] M. T. I. Rimon, M.W. Hasan, M. F. Hassan, S. Cesmeci, Advancements in Insulin Pumps: A Comprehensive Exploration of Insulin Pump Systems, Technologies, and Future Directions, *Pharmaceutics*, 2024, **16**, 944, doi: 10.3390/pharmaceutics16070944.
[17] N. N. L. Do, A. J. Taberner, B. P. Ruddy, Design of a portable pulsed power system for needle-free jet injection, 2018 IEEE Energy Conversion Congress and Exposition (ECCE), Portland, OR, USA. IEEE, 2018.
[18] J. C. Stachowiak, M. G. von Muhlen, T. H. Li, L. Jalilian, S. H. Parekh, D. A. Fletcher, Piezoelectric control of needle-free transdermal drug delivery, *Journal of Controlled Release*, 2007, **124**, 88-97, doi: 10.1016/j.jconrel.2007.08.017.
[19] M. A. Trimzi, Y.-B. Ham, B.-C. An, J.-H. Park, S.-N. Yun, Numerical analysis and simulation of an impulse driven piezoelectric needle-free jet injector, *Journal of Mechanical Science and Technology*, 2019, **33**, 3851-3858, doi: 10.1007/s12206-019-0728-9.
[20] Q. Yan, J. You, W. Sun, Y. Wang, H. Wang, L. Zhang, Advances in piezoelectric jet and atomization devices, *Applied Sciences*, 2021, **11**, 5093, doi: 10.3390/app11115093.
[21] H. Miyazaki, S. Atobe, T. Suzuki, H. Iga, K. Terai, Development of pyro-drive jet injector with controllable jet pressure, *Journal of Pharmaceutical Sciences*, 2019, **108**, 2415-2420, doi: 10.1016/j.xphs.2019.02.021.
[22] J. Sonoda, I. Mizoguchi, S. Inoue, A. Watanabe, A. Sekine, M. Yamagishi, S. Miyakawa, N. Yamaguchi, E. Horio, Y. Katahira, H. Hasegawa, T. Hasegawa, K. Yamashita, T. Yoshimoto, A promising needle-free pyro-drive jet injector for augmentation of immunity by intradermal injection as a physical adjuvant, *International Journal of Molecular Sciences*, 2023, **24**, 9094, doi: 10.3390/ijms24109094.
[23] A. Taberner, N. C. Hogan, I. W. Hunter, Needle-free jet injection using real-time controlled linear Lorentz-force actuators, *Medical Engineering & Physics*, 2012, **34**, 1228-1235, doi: 10.1016/j.medengphy.2011.12.010.
[24] J. H. Chang, N. C. Hogan, I. W. Hunter, A needle-free technique for interstitial fluid sample acquisition using a lorentz-force actuated jet injector, *Journal of Controlled Release*, 2015, **211**, 37-43, doi: 10.1016/j.jconrel.2015.05.264.
[25] G. Sripanagul, A. Matthujak, Fundamental study of electromagnetic actuated needle-free jet injection, *International Journal of Engineering & Technology*, 2018, **7**, 145, doi: 10.14419/ijet.v7i3.7.16258.
[26] G. Sripanagul, A. Matthujak, T. Sriveerakul, S. Phongthanapanich, Experimental investigation of stone drilling using water jet generated by electromagnetic actuator, *International Journal of Rock Mechanics and Mining Sciences*, 2021, **142**, 104697, doi: 10.1016/j.ijrmms.2021.104697.
[27] K.-J. Huang, C.-H. Li, P.-K. Tsai, C.-C. Lai, Y.-R. Kuo, M.-K. Hsieh, C.-W. Cheng, Electromagnetic force-driven needle-free in ovo injection device, *Veterinary Sciences*, 2022, **9**, 147, doi: 10.3390/vetsci9030147.
[28] A. Matthujak, C. Kasamnimitporn, T. Sriveerakul, Comparative visualized investigation of impact-driven high-speed liquid jets injected in submerged water and in ambient air, *Journal of Visualization*, 2020, **23**, 395-408, doi: 10.1007/s12650-020-00640-3.
[29] O. A. Shergold, N. A. Fleck, D. Radford, The uniaxial stress versus strain response of pig skin and silicone rubber at low and high strain rates, *International Journal of Impact Engineering*, 2006, **32**, 1384-1402, doi: 10.1016/j.ijimpeng.2004.11.010.
[30] A. Z. H. Tan, A. J. Taberner, J. W. McKeage, Rotatable orifice for needle-free jet injection, 2023 45th Annual International Conference of the IEEE Engineering in Medicine & Biology Society (EMBC). Sydney, Australia. IEEE, 2023.
[31] S. Mitragotri, Current status and future prospects of needle-free liquid jet injectors, *Nature Reviews Drug Discovery*, 2006, **5**, 543-548, doi: 10.1038/nrd2076.
[32] N. E. González-Sierra, J. M. Perez-Corte, J. P. Padilla-

Martinez, S. Cruz-Vanegas, S. Bonfadini, F. Storti, L. Criante, R. Ramos-García, Bubble dynamics and speed of jets for needle-free injections produced by thermocavitation, *Journal of Biomedical Optics*, 2023, **28**, 075004, doi: 10.1117/1.JBO.28.7.075004.
[33] X. Cheng, X.-P. Chen, H. Ding, C.-Y. Zhang, H. Hu, L. Jia, Viscous influences on impulsively generated focused jets, *Physical Review Fluids*, 2024, **9**, L082001, doi: 10.1103/physrevfluids.9.l082001.
[34] A. Matthujak, S. H. R. Hosseini, K. Takayama, M. Sun, P. Voinovich, High speed jet formation by impact acceleration method, *Shock Waves*, 2007, **16**, 405-419, doi: 10.1007/s00193-007-0079-9.